Supporting information

Coupled motion in proteins revealed by pressure perturbation

Yinan Fu,[†] Vignesh Kasinath,[†] Veronica R. Moorman,[†] Nathaniel V. Nucci,[†] Vincent J. Hilser[‡] & A. Joshua Wand[†*]

[†] Graduate Group in Biochemistry and Molecular Biophysics and Department of Biochemistry & Biophysics, University of Pennsylvania, Philadelphia, Pennsylvania 19104 USA

[‡] Department of Biology, Johns Hopkins University, Baltimore, Maryland 21218 USA

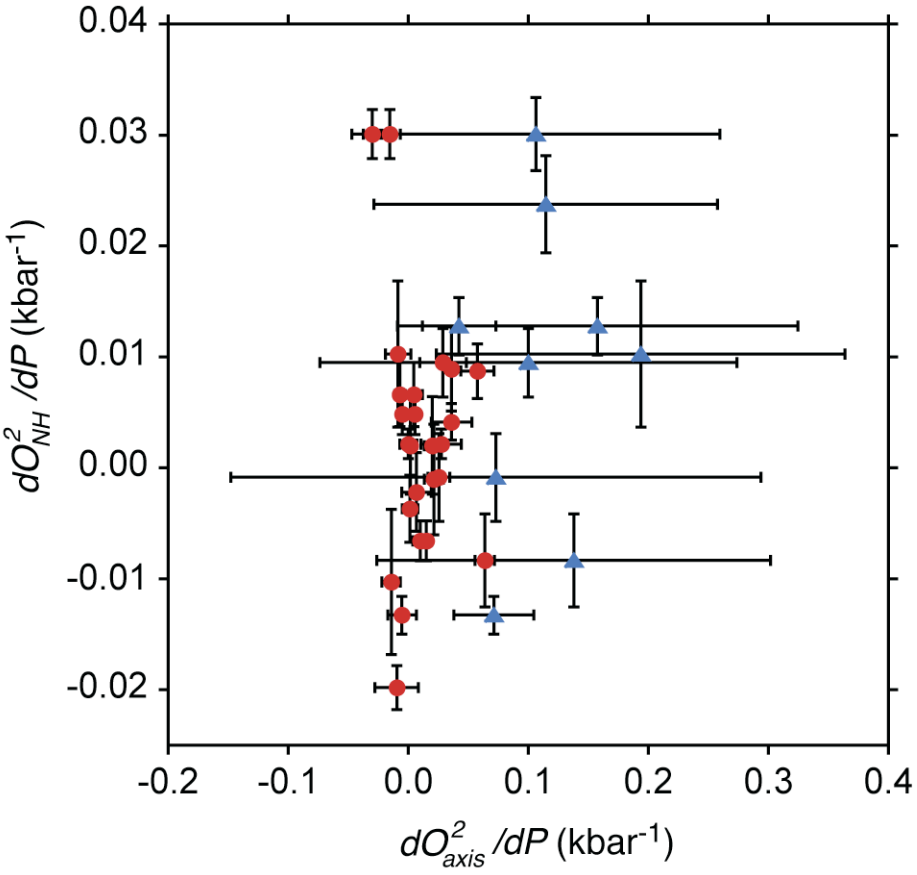

Figure S1. The pressure sensitivity of backbone and methyl-bearing side chain motion is uncorrelated ($R < 0.03$). Solid red circles and solid blue triangles correspond to methyls with a purely linear pressure response and those with a non-linear pressure response, respectively. For the latter, the first order term from the fitted Taylor expansion is used, which have generally lower precision than that derived from the purely linear response sites. The lack of correlation indicates that the motion of the main chain and methyl-bearing side chains are largely decoupled.

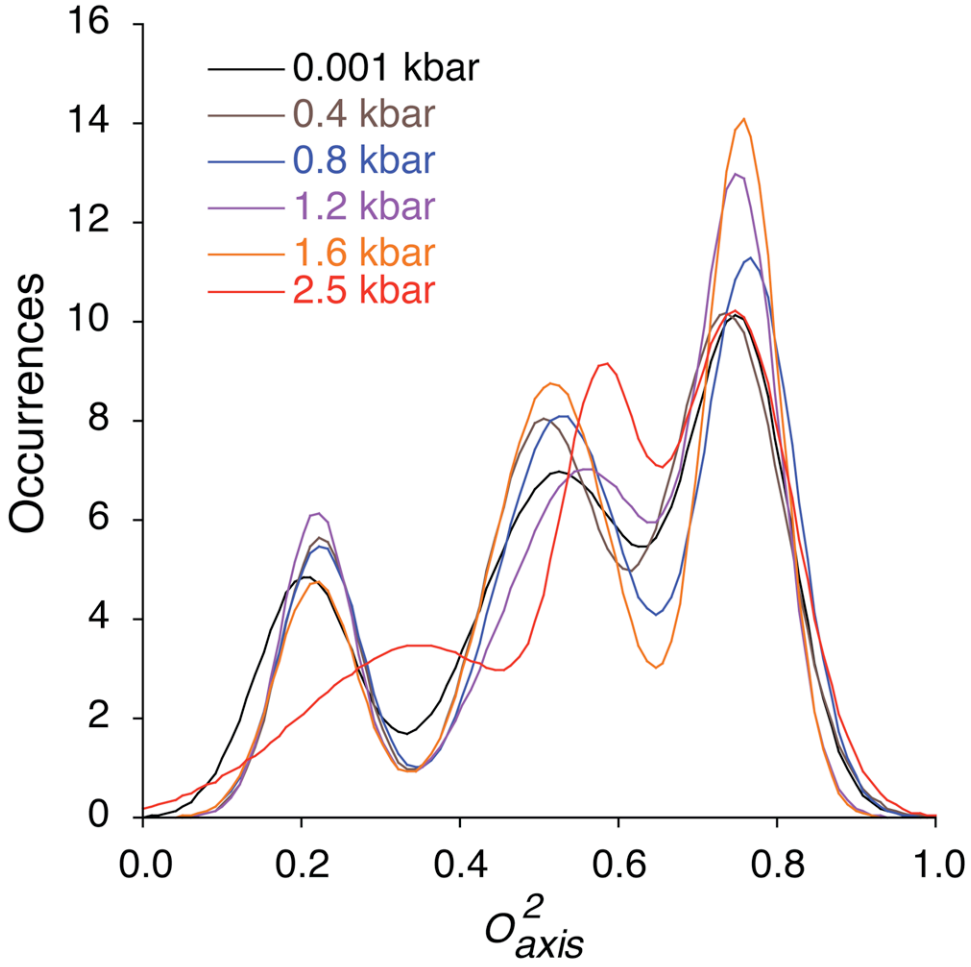

Figure S2. Overlay of fitted tri-Gaussian distributions of the methyl symmetry axis squared generalized order parameter at 0.001, 0.4, 0.8, 1.2, 1.6 and 2.5 kbar. The fitting parameters and statistics are listed in Table S4.

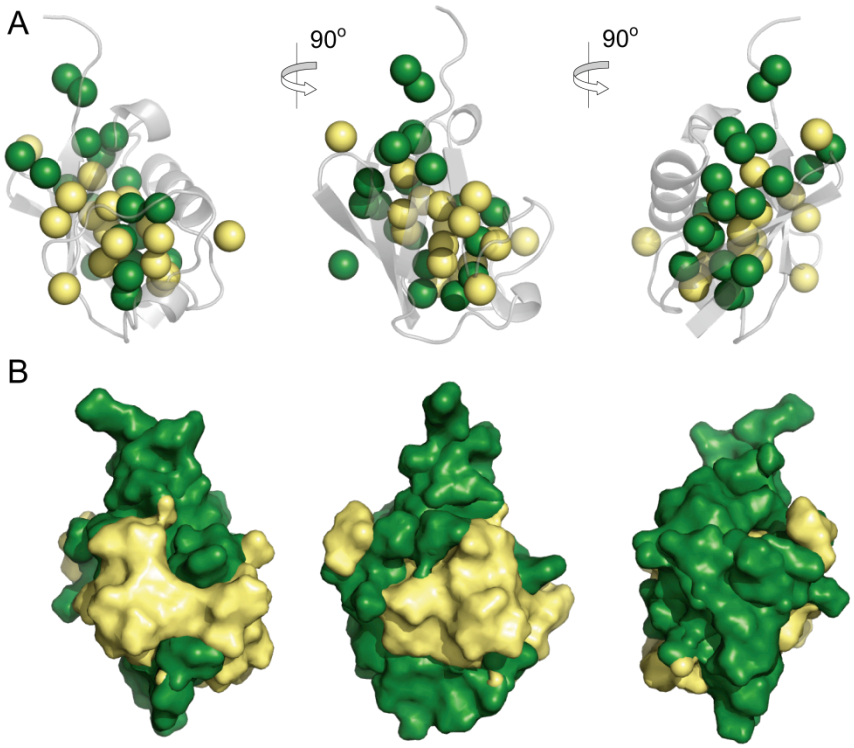

Figure S3. (A) Spatial distribution of methyl bearing side chains that have linear relation between O^2_{axis} and dO^2_{axis}/dP (yellow) and the remaining methyls (green). Exhaustive randomization statistical tests confirm that the groups (excluding L73δ2) are spatially clustered within the molecular structure ($p < 0.01$). **(B)** Each atom including added hydrogens in the 1 bar crystal structure (PDB 1UBQ) was assigned to a group based on the group identity of the nearest analyzed probe's methyl carbon. Surface renderings were made for each cluster and colored accordingly. Hydrogen atoms were added and molecular images were generated using PyMOL.

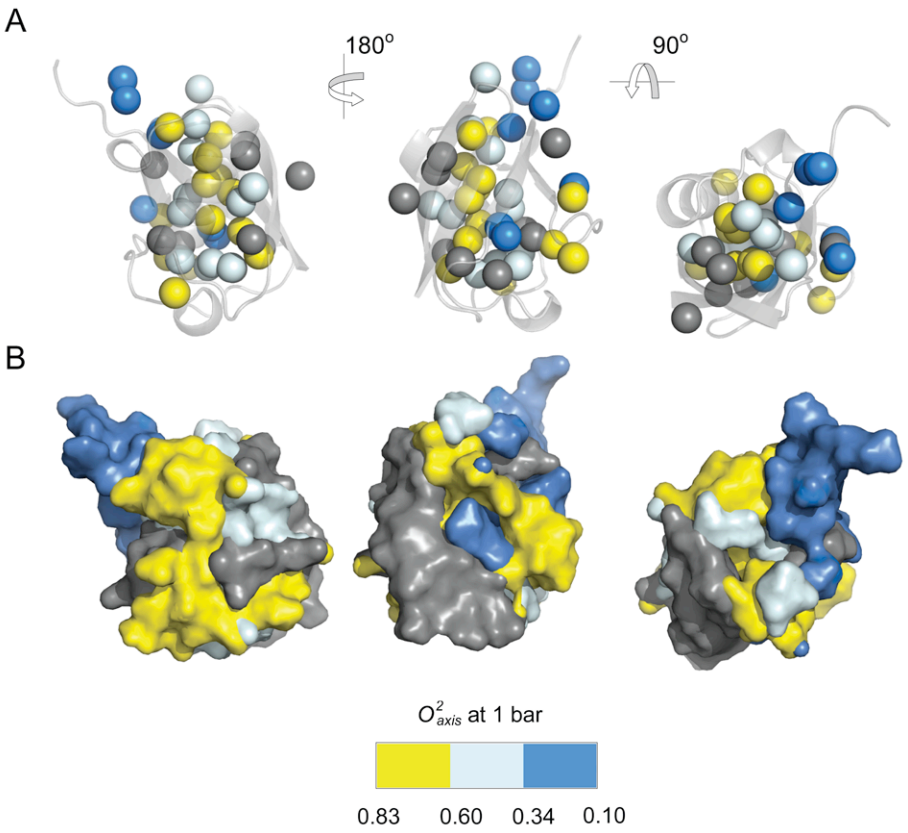

Figure S4. Spatial clustering of fast methyl side chain motion in ubiquitin at ambient pressure. A) Different orientations of the crystal structure of ubiquitin (PDB 1UBQ) represented as a ribbon with side chain methyl carbons shown as spheres and colored (see the color bar) according to their membership in three groups derived from a k-means analysis of O^2_{axis} values at 1 bar (see Methods). The methyls that do not have a linear dynamic response to pressure were grouped separately and are colored gray. Exhaustive randomization statistical tests confirm that the groups (excluding T22γ2 and A46β) are spatially clustered within the molecular structure ($p < 0.05$). These regions are emphasized in B) where each atom including added hydrogens in the crystal structure (PBD 1UBQ) was assigned to a group based on the group identity of the nearest analyzed methyl carbon probe. Surface renderings were made for each group and colored accordingly. Hydrogen atoms were added and molecular images were generated using PyMOL.

Table S1. Pressure dependence of ubiquitin backbone amide N-H squared generalized order parameters.[a]

ID	O^2_{NH} at 0.001 kbar	O^2_{NH} at 0.4 kbar	O^2_{NH} at 0.8 kbar	O^2_{NH} at 1.2 kbar	O^2_{NH} at 1.6 kbar	O^2_{NH} at 2.5 kbar	dO^2_{NH}/dP $\times 10^3$ (kbar^{-1})
Q2	0.79±0.011	0.86±0.008	0.86±0.002	0.87±0.003	0.87±0.004	0.86±0.006	2.7±3.2
I3	0.87±0.004	0.90±0.008	0.90±0.006	0.91±0.004	0.90±0.003	0.93±0.006	9.5±3.1
F4	0.81±0.004	n.d.[b]	n.d.	0.91±0.005	0.92±0.004	0.93±0.006	2.3±3.1
V5	0.76±0.008	0.82±0.005	0.85±0.003	0.84±0.005	0.85±0.004	0.84±0.007	6.6±2.9
K6	0.75±0.006	0.83±0.006	0.76±0.011	0.88±0.004	0.87±0.005	0.93±0.010	58.0±4.8
T7	0.70±0.008	0.86±0.005	0.87±0.003	0.89±0.005	0.87±0.006	n.d.	8.9±3.8
L8	0.77±0.005	0.81±0.006	0.85±0.004	0.84±0.004	0.82±0.005	0.83±0.005	8.7±2.5
T9	0.85±0.006	0.75±0.008	0.78±0.005	0.79±0.004	0.75±0.006	0.75±0.007	-2.2±3.6
G10	0.84±0.005	0.69±0.012	0.78±0.002	0.77±0.001	0.74±0.005	0.76±0.006	11.6±3.4
K11	0.85±0.002	0.73±0.006	0.74±0.007	0.73±0.008	0.70±0.008	0.71±0.016	-0.9±6.1
T12	0.90±0.004	0.77±0.007	0.77±0.005	0.79±0.007	0.79±0.006	n.d.	13.7±4.4
I13	0.86±0.001	0.86±0.008	n.d.	n.d.	0.86±0.004	0.89±0.004	12.8±2.6
T14	0.86±0.002	0.85±0.006	0.87±0.004	0.87±0.002	0.88±0.004	n.d.	30.1±3.3
L15	n.d.	0.87±0.003	0.87±0.003	0.91±0.002	0.90±0.003	n.d.	30.1±2.2
V17	0.87±0.004	0.89±0.003	0.90±0.004	n.d.	n.d.	n.d.	10.3±6.6
E18	0.97±0.009	n.d.	n.d.	0.87±0.004	0.89±0.004	0.87±0.004	5.1±1.5
S20	0.90±0.004	0.85±0.006	0.86±0.004	0.88±0.005	0.87±0.008	0.85±0.005	0.1±2.4
D21	0.91±0.005	0.93±0.005	0.96±0.006	0.94±0.005	0.99±0.009	0.93±0.006	1.3±3.4
T22	n.d.	0.86±0.004	0.89±0.005	0.85±0.009	0.86±0.007	0.86±0.007	-3.7±3.0
I23	0.94±0.003	0.97±0.006	0.96±0.007	0.96±0.003	0.97±0.007	0.97±0.008	-0.9±3.9
V26	0.90±0.004	0.90±0.006	0.89±0.003	n.d.	n.d.	n.d.	0.0±18.1
K27	0.91±0.002	0.95±0.004	0.87±0.005	n.d.	0.98±0.005	0.94±0.004	-10.3±6.5
A28	0.93±0.005	0.95±0.004	0.94±0.005	0.94±0.003	0.97±0.004	0.96±0.004	17.9±2.3
K29	0.84±0.005	0.90±0.005	0.86±0.007	0.92±0.003	0.95±0.003	0.92±0.004	10.5±2.7
I30	0.89±0.004	0.92±0.003	0.91±0.003	0.91±0.005	0.91±0.004	0.92±0.004	6.4±2.0
D32	0.80±0.006	0.93±0.004	0.91±0.003	0.91±0.003	0.93±0.004	0.93±0.003	4.8±1.9
K33	0.87±0.002	0.85±0.005	0.83±0.008	0.85±0.006	0.82±0.009	0.95±0.004	6.4±1.5
E34	0.88±0.004	0.85±0.005	0.85±0.004	0.86±0.004	0.86±0.004	0.88±0.006	10.8±2.5
G35	0.88±0.002	0.91±0.005	0.92±0.006	0.90±0.003	0.91±0.005	0.91±0.003	16.9±2.6
I36	0.85±0.002	0.80±0.007	0.80±0.008	0.79±0.010	0.83±0.007	0.79±0.010	7.0±1.9
D39	0.86±0.003	0.90±0.002	0.90±0.004	n.d.	n.d.	0.91±0.007	2.0±4.4

Q40	0.84±0.004	0.89±0.006	0.90±0.003	0.89±0.001	0.91±0.004	0.90±0.003	14.5±2.9
Q41	0.76±0.006	0.88±0.002	0.88±0.002	0.88±0.002	0.88±0.004	0.88±0.002	6.1±1.8
I44	0.87±0.004	0.87±0.002	0.86±0.002	0.87±0.001	0.86±0.003	0.87±0.003	1.4±1.1
A46	0.81±0.007	0.90±0.005	0.86±0.004	0.87±0.005	0.82±0.004	0.83±0.004	2.1±1.3
G47	0.86±0.005	0.85±0.003	0.84±0.002	0.86±0.002	0.84±0.002	0.84±0.003	-19.8±2.0
Q49	0.88±0.005	0.78±0.006	0.76±0.008	0.78±0.004	0.79±0.005	0.79±0.003	-1.5±1.6
L50	0.93±0.005	0.86±0.003	0.87±0.004	0.87±0.003	0.85±0.004	0.83±0.004	10.0±2.3
D52	0.90±0.002	0.80±0.006	0.81±0.007	0.82±0.006	0.82±0.006	0.82±0.005	-13.3±1.7
R54	0.93±0.004	0.88±0.004	0.89±0.004	0.88±0.002	0.91±0.004	0.88±0.004	8.4±2.9
T55	0.85±0.004	0.90±0.007	0.91±0.003	0.90±0.002	0.90±0.003	0.90±0.002	9.8±1.9
L56	0.88±0.003	0.94±0.005	0.94±0.002	0.91±0.003	0.92±0.004	0.92±0.002	2.4±2.0
S57	n.d.	0.90±0.002	0.91±0.003	n.d.	n.d.	0.90±0.003	-6.6±1.8
D58	0.73±0.010	0.90±0.003	0.92±0.003	0.92±0.002	0.93±0.003	0.90±0.002	-1.3±1.4
Y59	0.83±0.006	0.87±0.003	0.85±0.006	0.87±0.004	0.85±0.004	0.87±0.003	-6.9±1.5
N60	0.89±0.011	0.90±0.004	0.89±0.003	0.91±0.009	0.90±0.007	0.91±0.009	5.5±1.6
I61	0.87±0.003	n.d.	n.d.	0.90±0.003	0.91±0.004	0.89±0.005	6.4±3.5
Q62	0.86±0.003	0.75±0.013	0.73±0.014	0.73±0.014	0.74±0.011	0.72±0.013	-8.3±4.2
K63	0.87±0.002	0.86±0.004	0.85±0.004	0.85±0.006	0.91±0.005	0.87±0.007	-4.9±6.0
E64	0.87±0.002	0.91±0.009	0.90±0.003	0.91±0.004	0.88±0.006	0.92±0.005	19.5±3.2
S65	0.91±0.004	0.89±0.004	0.90±0.002	0.90±0.003	0.88±0.002	0.88±0.003	5.3±3.9
T66	0.79±0.011	0.84±0.004	0.87±0.004	0.87±0.006	0.85±0.004	n.d.	-0.1±1.6
L67	0.87±0.004	0.87±0.002	n.d.	n.d.	0.86±0.005	0.88±0.004	4.1±3.5
H68	0.81±0.004	0.88±0.004	0.87±0.00	0.84±0.004	0.90±0.004	0.89±0.003	4.1±1.6
V70	0.76±0.008	0.92±0.005	0.95±0.01	0.98±0.014	0.97±0.011	0.96±0.010	7.4±1.5
L71	0.75±0.006	0.86±0.005	0.83±0.01	0.84±0.011	0.87±0.010	0.84±0.009	23.8±4.4

[a] Rotational diffusion tensors were determined using the statistical analysis of the ^{15}N relaxation data largely as suggested by Bax and coworkers (19) with small modification of the reduced fitting error function (see Methods). The ambient pressure crystal structure (1UBQ) was used for data collected at 1, 400 and 800 bar. The high-pressure solution structure (1V81) was used for higher pressures. A grid search method with local refinement of model-free parameters was employed (40). A fully anisotropic diffusion model was statistically warranted for data at all pressures ($p < 0.05$). The anisotropy ($2D_z/[D_x+D_y]$) was 1.085 or less at all pressures. Those amides whose signals cannot be satisfactorily resolved in relaxation spectra at the given pressure are designated as 'not determined' (n.d.). Errors were determined by Monte Carlo sampling of observed T_1, T_2 and NOE values based on errors estimated from replicate sampling and noise estimation.

Table S2. Pressure dependence of ubiquitin methyl symmetry axis squared generalized order parameters. [a]

ID	O^2_{axis} at 0.001 kbar	O^2_{axis} at 0.4 kbar	O^2_{axis} at 0.8 kbar	O^2_{axis} at 1.2 kbar	O^2_{axis} at 1.6 kar	O^2_{axis} at 2.5 kbar
I3δ1	0.651±0.014	0.663±0.040	0.665±0.045	0.718±0.039	0.705±0.040	0.717±0.047
I3γ2	0.818±0.006	0.835±0.052	0.832±0.054	0.787±0.049	0.778±0.047	0.810±0.053
V5γ1	0.754±0.024	0.768±0.008	0.756±0.007	0.767±0.007	0.742±0.002	0.778±0.004
V5γ2	0.736±0.010	0.750±0.008	0.736±0.007	0.742±0.004	0.725±0.004	0.726±0.007
T7γ2	0.734±0.005	0.707±0.006	0.756±0.002	0.762±0.002	0.786±0.005	0.806±0.001
L8δ1	0.209±0.002	0.235±0.041	0.243±0.039	0.282±0.037	0.285±0.037	0.358±0.030
T9γ2	0.586±0.035	0.576±0.011	0.594±0.012	0.599±0.014	0.590±0.015	0.600±0.022
I13δ1	0.475±0.012	0.493±0.007	0.508±0.007	0.514±0.006	0.512±0.005	0.520±0.018
I13γ2	0.514±0.020	0.568±0.012	0.570±0.012	0.569±0.011	0.572±0.010	0.617±0.034
T14γ2	0.614±0.013	0.633±0.011	0.629±0.010	0.599±0.013	0.580±0.010	0.610±0.006
L15δ1	0.457±0.002	0.443±0.010	0.463±0.008	0.395±0.026	0.415±0.023	0.388±0.019
L15δ2	0.449±0.018	0.463±0.015	0.465±0.016	0.425±0.024	0.421±0.024	0.427±0.017
V17γ1	0.764±0.003	0.800±0.028	0.818±0.028	0.787±0.023	0.754±0.027	0.782±0.032
V17γ2	0.750±0.003	0.750±0.023	0.770±0.025	0.762±0.026	0.740±0.026	0.732±0.026
T22γ2	0.802±0.022	0.867±0.007	0.853±0.006	0.846±0.005	0.847±0.006	0.828±0.005
I23δ1	0.455±0.016	0.485±0.022	0.489±0.022	0.500±0.023	0.505±0.020	0.526±0.019
I23γ2	0.748±0.033	0.760±0.008	0.762±0.007	0.737±0.007	0.726±0.006	0.740±0.005
V26γ1	0.756±0.007	0.762±0.022	0.754±0.021	0.767±0.021	0.748±0.020	0.721±0.015
I30δ1	0.685±0.004	0.699±0.006	0.695±0.006	0.708±0.004	0.719±0.003	0.695±0.005
I30γ2	0.830±0.010	0.841±0.007	0.816±0.007	0.851±0.004	0.837±0.007	0.814±0.008
I36δ1	0.477±0.003	0.493±0.018	0.499±0.016	0.524±0.017	0.491±0.020	0.536±0.013
I36γ2	0.740±0.002	0.728±0.011	0.742±0.009	0.737±0.008	0.719±0.009	0.748±0.006
L43δ1	0.568±0.009	0.554±0.006	0.524±0.005	0.604±0.006	0.540±0.005	0.508±0.006
L43δ2	0.449±0.027	0.441±0.022	0.455±0.022	0.445±0.026	0.461±0.023	0.459±0.022
I44δ1	0.195±0.048	0.201±0.030	0.205±0.027	0.222±0.031	0.231±0.030	0.263±0.021
I44γ2	0.629±0.005	0.649±0.018	0.621±0.016	0.653±0.018	0.641±0.016	0.631±0.016
A46β	0.780±0.005	0.790±0.048	0.786±0.047	0.782±0.042	0.760±0.043	0.766±0.042
L50δ1	0.693±0.013	0.689±0.005	0.707±0.007	0.698±0.004	0.721±0.007	0.608±0.007
L50δ2	0.671±0.007	0.695±0.008	0.701±0.007	0.698±0.008	0.667±0.008	0.673±0.033

L56δ1	0.534±0.007	0.546±0.012	0.580±0.010	0.609±0.011	0.524±0.017	0.590±0.006
L56δ2	0.524±0.007	0.550±0.021	0.546±0.021	0.589±0.022	0.552±0.023	0.554±0.009
I61δ1	0.505±0.025	0.536±0.004	0.576±0.004	0.604±0.004	0.612±0.009	0.667±0.010
I61γ2	0.719±0.016	0.762±0.019	0.752±0.021	0.752±0.013	0.736±0.016	0.774±0.018
L67δ1	0.243±0.037	0.259±0.024	0.261±0.041	0.291±0.035	0.286±0.037	0.336±0.033
L67δ2	0.233±0.022	0.257±0.040	0.267±0.044	0.291±0.044	0.302±0.041	0.324±0.041
L69δ2	0.526±0.012	0.546±0.023	0.540±0.011	0.564±0.022	0.495±0.016	0.560±0.019
V70γ2	0.336±0.034	0.368±0.011	0.395±0.012	0.400±0.013	0.411±0.008	0.455±0.008
L71δ1	0.233±0.002	0.241±0.023	0.241±0.014	0.262±0.015	0.265±0.015	0.285±0.019
L73δ1	0.108±0.029	0.116±0.022	0.106±0.023	0.123±0.031	0.124±0.031	0.128±0.012
L73δ2	0.144±0.011	0.156±0.011	0.158±0.007	0.138±0.031	0.140±0.026	0.150±0.035

[a] Calculated using the appropriate macromolecular diffusion tensor determined by ^{15}N relaxation (see Table S1). Errors were determined by Monte Carlo sampling of T_1 and $T_{1\rho}$ based on errors estimated from replicate sampling.

Table S3. Pressure dependence of the 3-Gaussian distribution of methyl symmetry axis squared generalized order parameters in ubiquitin.[a]

	Fitted parameters	Pressure (kbar) 0.001	0.4	0.8	1.2	1.6	2.5
J-class	J_A	4.82±3.31	5.65±7.71	5.47±2.11	6.13±1.00	4.75±0.88	3.47±1.23
	J_0	0.21±0.03	0.22±0.09	0.22±0.03	0.22±0.01	0.22±0.01	0.35±0.20
	J	0.09±0.10	0.07±0.13	0.07±0.04	0.07±0.01	0.07±0.02	0.21±0.22
α-class	α_A	6.96±1.38	7.98±3.49	8.10±1.33	7.02±0.08	8.78±0.42	7.41±18.01
	α_0	0.53±0.07	0.51±0.02	0.53±0.04	0.56±0.01	0.52±0.00	0.58±0.19
	α	0.14±0.13	0.10±0.12	0.11±0.07	0.15±0.02	0.11±0.01	0.07±0.16
ω-class	ω_A	9.56±3.13	10.15±1.13	11.20±1.48	11.81±0.58	14.05±0.26	10.10±1.77
	ω_0	0.75±0.05	0.74±0.03	0.77±0.04	0.76±0.01	0.76±0.01	0.75±0.16
	ω	0.09±0.04	0.10±0.03	0.08±0.04	0.07±0.01	0.07±0.01	0.11±0.15
	R	0.99	0.99	0.99	1	1	0.99

[a] The fitting function is

$$Occurences(O^2_{axis}) = J_A \times \exp(-(x - J_0)^2 / J^2) + \alpha_A \times \exp(-(x - \alpha_0)^2 / \alpha^2) + \omega_A \times \exp(-(x - \omega_0)^2 / \omega^2)$$

where J_A, α_A and ω_A are the amplitudes; J_0, α_0 and ω_0 are the centers; J, α, ω are the widths of the J, α and ω–classes, respectively. KaleidaGraph was used for curve fitting and regression error analysis.

Table S4. Pressure dependence of methyl symmetry axis squared generalized order parameters of ubiquitin.[a]

ID	Degree of Polynomial	First Order ($kbar^{-1}$)	Second Order[b] ($kbar^{-2}$)	Third Order[b] ($kbar^{-3}$)	R	p_{3v1}[c]	p_{2v1}[c]	p_{3v2}[c]
I3δ1	1	0.0289±0.0195	n.a.	n.a.	0.87	0.43	0.37	0.59
I3γ2	3	0.0998±0.1739	-0.150±0.061	0.043±0.026	0.96	0.05	0.47	0.06
V5γ1	1	0.0047±0.007	n.a.	n.a.	0.33	0.20	0.48	0.23
V5γ2	1	-0.0072±0.0039	n.a.	n.a.	0.67	0.31	0.74	0.29
T7γ2	1	0.0359±0.0019	n.a.	n.a.	0.91	0.42	n.a.	0.36
L8δ1	1	0.0576±0.0139	n.a.	n.a.	0.98	0.43	0.35	0.60
T9γ2	1	0.0069±0.0123	n.a.	n.a.	0.69	0.94	0.80	0.91
I13δ1	2	0.0425±0.0306	-0.010±0.013	n.a.	0.98	0.03	0.04	0.14
I13γ2	3	0.1579±0.1667	-0.135±0.042	0.035±0.019	0.99	0.05	0.81	0.05
T14γ2	3	0.1062±0.1532	-0.145±0.033	0.041±0.013	0.99	0.01	0.61	0.01
L15δ1	1	-0.0297±0.0076	n.a.	n.a.	0.83	0.85	0.90	0.72
L15δ2	1	-0.0155±0.0088	n.a.	n.a.	0.94	0.13	0.88	0.13
V17γ1	3	0.1934±0.1703	-0.208±0.041	0.054±0.018	0.97	0.03	0.69	0.03
V17γ2	1	-0.0086±0.0106	n.a.	n.a.	0.57	0.24	0.21	0.46
T22γ2	1	0.0015±0.0064	n.a.	n.a.	0.05	0.12	0.18	0.24
I23δ1	1	0.0255±0.0093	n.a.	n.a.	0.96	0.11	0.29	0.16
I23γ2	3	0.0725±0.2207	-0.096±0.052	0.027±0.019	0.97	0.04	0.78	0.04
V26γ1	1	-0.0142±0.0077	n.a.	n.a.	0.77	0.14	0.06	0.89
I30δ1	1	0.0054±0.0023	n.a.	n.a.	0.41	0.10	0.09	0.33
I30γ2	1	-0.005±0.0039	n.a.	n.a.	0.30	0.46	0.37	0.63
I36δ1	1	0.0199±0.0064	n.a.	n.a.	0.79	0.50	n.a.	0.42
I36γ2	1	0.0018±0.0032	n.a.	n.a.	0.14	0.35	0.36	0.47
L43δ1	1	-0.0181±0.0036	n.a.	n.a.	0.48	0.59	0.54	0.63
L43δ2	1	0.0059±0.0117	n.a.	n.a.	0.66	0.65	0.92	0.55
I44δ1	1	0.0275±0.0168	n.a.	n.a.	0.98	0.11	0.06	0.53
I44γ2	1	0.0001±0.0071	n.a.	n.a.	0.00	0.72	0.52	0.89
A46β	1	-0.0095±0.0181	n.a.	n.a.	0.73	0.08	0.81	0.08
L50δ1	2	-0.0431±0.0333	-0.039±0.013	n.a.	0.98	0.03	0.06	0.13
L50δ2	1	-0.0052±0.0119	n.a.	n.a.	0.32	0.06	0.34	0.08

L56δ1	1	0.0153±0.0042	n.a.	n.a.	0.40	0.49	0.77	0.43
L56δ2	1	0.0100±0.0061	n.a.	n.a.	0.44	0.35	0.21	0.77
I61δ1	1	0.0637±0.008	n.a.	n.a.	0.98	0.17	0.14	0.43
I61γ2	3	0.1374±0.164	-0.139±0.037	0.037±0.015	0.97	0.05	0.92	0.05
L67δ1	1	0.036±0.0169	n.a.	n.a.	0.98	0.59	0.46	0.71
L67δ2	1	0.0364±0.018	n.a.	n.a.	0.98	0.15	0.07	0.79
L69δ2	1	0.0046±0.0087	n.a.	n.a.	0.17	0.32	0.79	0.30
V70γ2	3	0.1148±0.1432	-0.069±0.045	0.017±0.016	0.98	0.05	0.40	0.07
L71δ1	1	0.0212±0.0079	n.a.	n.a.	0.98	0.73	0.80	0.63
L73δ1	1	0.0083±0.0108	n.a.	n.a.	0.83	0.14	0.78	0.13
L73δ2	1	-0.0016±0.0137	n.a.	n.a.	0.17	0.79	0.88	0.67

[a] O^2_{axis} against pressure was fitted using KaleidaGraph. Errors were estimated from Monte Carlo sampling. Quadratic and cubic terms for data that do not require second or third order curve fitting are designated as 'not applicable' (n.a.).

[b] Raw fitted coefficients are listed i.e. not corrected for the leading (1/2) and (1/6) factors of the Taylor series expansion

[c] The best fitting polynomial model for each methyl was determined by pair wise comparison of statistic p values of cubic verse linear (p_{3v1}), quadratic versus linear (p_{2v1}) and cubic versus quadratic (p_{3v2}) (see Methods). The p-value entries shown as 'not applicable' (n.a.) correspond to sites with negative F-values.

Table S5. Summary of pressure dependence of methyl side chain dynamics in ubiquitin.

Linear Response to Pressure			Non-linear Response to Pressure	
Linear [a]	Outliers [b]	Structural Change [c]	Structural Change[c]	Others
V5γ1, V5γ2, T9γ2, V17γ2, T22γ2, I23δ1, V26δ1, I30δ1, L43δ2, I44δ1, I44γ2, A46β, L50δ2, L56δ1, L56δ2, L67δ1, L67δ2, L69δ2	I3δ1, T7γ2, L8δ1, L15δ1, I61δ1, L73δ1	L15δ2, I30γ2, I36δ1, I36γ2, L43δ1, L71δ1, L73δ2	I13δ1, T14γ2, V70γ2	I3γ2, I13γ2, V17γ1, I23γ2, L50δ1, I61γ2

[a] Corresponding to the eighteen sites that have a linear correlation between O^2_{axis} at 1 bar and dO^2_{axis}/dP ($R > 0.9$) as seen in Fig. 4.

[b] The six methyls identified as outliers in Fig 4.

[c] Methyls that are experiencing significant pressure-induced structural change determined by superimposition of the 1 bar crystal structure (1UBQ) upon the ten models of 3 kbar NMR structure ensemble (1V81). Methyls that have a structural change greater than 3 Å in at least 5 out of total 10 compared structure pairs were considered to have significant structural change.

Table S6. Numerical grouping of the methyl-bearing side chains of ubiquitin according to the values of their methyl symmetry axis order parameters at 1 bar and their corresponding pressure sensitivity. [a]

Parameter	Group 1	Group 2	Group 3	Group 4	Group 5
O^2_{axis} at 1 bar	I3γ2, T14γ2, I13δ1, I13γ2, V17γ1, I23γ2, L50δ1, I61γ2, V70γ2	I3δ1, V5γ1, V5γ2, T7γ2, V17γ2, T22γ2, V26γ1, I30δ1, I30γ2, I36γ2, I44γ2, A46β, L50δ2	T9γ2, L15δ1, L15δ2, I23δ1, I36δ1, L43δ1, L43δ2, L56δ1, L56δ2, I61δ1, L69δ2	L8δ1, I44δ1, L67δ1, L67δ2, L71δ1, L73δ1, L73δ2	
dO^2_{axis}/dP		V5γ2, L15δ1, L15δ2, V17γ2, V26γ1, I30γ2, L43δ1, A46β, L50δ2	V5γ1, T9γ2, T22γ2, I30δ1, I36γ2, L43δ2, I44γ2, L56δ1, L56δ2, L69δ2, L73δ1, L73δ2	I3δ1, T7γ2, I23δ1, I36δ1, I44δ1, L67δ1, L67δ2, L71δ1	L8δ1, I61δ1

[a] Methyls that have a non-linear pressure sensitivity are grouped in group 1. The remaining methyls were numerically grouped into 4 sets based on their dO^2_{axis}/dP values and into 3 groups based on their O^2_{axis} parameters seen at ambient pressure. These groups were then subjected to spatial clustering analysis.